

Lithium-Ion Battery End-of-Discharge Time Estimation and Prognosis based on Bayesian Algorithms and Outer Feedback Correction Loops: A Comparative Analysis

Carlos Tampier¹, Aramis Pérez¹, Francisco Jaramillo¹, Vanessa Quintero¹, Marcos E. Orchard¹ and Jorge F. Silva¹

¹*Department of Electrical Engineering, Universidad de Chile, Santiago 8370451, Chile*

ctampier@ing.uchile.cl,

aramis.perez@ing.uchile.cl

vquintero@ing.uchile.cl

francisco.jaramillo@ing.uchile.cl

morchard@ing.uchile.cl

josilva@ing.uchile.cl

ABSTRACT

Battery energy systems are currently one of the most common power sources found in mobile electromechanical devices. In all these equipment, assuring the autonomy of the system requires to determine the battery state-of-charge (SOC) and predicting the end-of-discharge time with a high degree of accuracy. In this regard, this paper presents a comparative analysis of two well-known Bayesian estimation algorithms (Particle filter and Unscented Kalman filter) when used in combination with Outer Feedback Correction Loops (OFCLs) to estimate the SOC and prognosticate the discharge time of lithium-ion batteries. Results show that, on the one hand, a PF-based estimation and prognosis scheme is the method of choice if the model for the dynamic system is inexact to some extent; providing reasonable results regardless if used with or without OFCLs. On the other hand, if a reliable model for the dynamic system is available, a combination of an Unscented Kalman Filter (UKF) with OFCLs outperforms a scheme that combines PF and OFCLs.

1. INTRODUCTION

The main focus of this research is to establish a comparative analysis of two well-known Bayesian estimation algorithms, particle-filter (PF) (Arulampalam, Maskell, Gordon & Clapp) and UKF (Partovibakhsh & Guaniun, 2015), when used in combination with OFCLs (Orchard, Kacprzyński, Goebel, Saha & Vachtsevanos, 2008),

(Orchard, 2007) to estimate the SOC and prognosticate the end-of-discharge (EoD) time of lithium-ion batteries.

The proposed case study, which is related to the problem of autonomy assessment in electromechanical devices, is selected due to its importance in decision-making processes that are related to mission reformulation based on condition monitoring, where the availability of real-time information is critical for optimal performance. Even though many manufacturers provide detailed information for batteries operating at constant temperatures and/or discharge currents, in practice this information is insufficient to avoid considerable errors on the autonomy estimates of the devices under time-varying power demands.

Numerous research efforts (Pola, Navarrete, Orchard, Rabie, Cerda, Olivares, Silva, Espinoza & Perez, 2015) have identified advantages associated with the implementation of Bayesian estimation techniques such as PF or UKF to characterize process and measurement uncertainty in the aforementioned problem. However, the incorporation of OFCLs has not been sufficiently discussed. In this regard, this article intends to present scientific evidence that could help future researchers to assess the real value behind the implementation of these schemes to characterize the uncertainty associated with the state estimates; which in turn define all initial conditions for online prognosis modules.

The structure of the article is as follows. Section 2 focuses on describing the theoretical framework that is required to understand the research performed. Section 3 presents the manner in which PF, UKF, and OFCLs algorithms were implemented to solve the SOC estimation problem. Section 4 presents the obtained results in terms of state estimation and EoD prognosis stages. Section 5 focuses on providing a performance comparison in terms of adequate

Carlos Tampier et al. This is an open-access article distributed under the terms of the Creative Commons Attribution 3.0 United States License, which permits unrestricted use, distribution, and reproduction in any medium, provided the original author and source are credited.

measures, and finally Section 6 summarizes the main conclusions of this research effort.

2. THEORETICAL FRAMEWORK

2.1. Outer Feedback Correction Loops

OFCLs play an important role within the structure of online prognosis modules, since they are capable of assuring increased precision and accuracy of remaining useful life (RUL) estimates model (Orchard, 2008). Typically, they measure the prediction capability offered by the process model (Orchard, 2008), (Orchard, 2007) through the analysis of short term prediction errors, improving the performance of the prognosis algorithm by either modifying the structure of the model that is used during the filtering stage (Orchard, Tobar, Vachtsevanos, 2009) or updating the hyper-parameters that define the process or observation noises (Orchard, et al., 2008), (Orchard, 2007), (Cruse, 2004).

One example of OFCLs is found in (Orchard, et al. 2009), where the authors propose a method that modifies the process noise variance depending if the prediction error over a horizon s , starting from a time t , $e^s(t)$, is bigger or smaller than a determined threshold e^{th} . Equation (1) shows the rule of decision, where $[p, q]$ are such that, $0 < p < 1$ and $1 < q$. As a result, the process variance related to the artificial evolution equation (Orchard, 2009) will increase if the prediction quality over the short-term horizon is poor, or it will decrease otherwise.

$$\text{var}(w(t)) = \begin{cases} p \cdot \text{var}(w(t)), & |e^s(t)| \leq e^{th} \\ q \cdot \text{var}(w(t)), & |e^s(t)| > e^{th} \end{cases} \quad (1)$$

2.2. Prognosis Performance Indices

The evaluation of an algorithm capacity to predict the time-of-failure (ToF), which in this case would be equivalent to the EoD time, can be done considering different characteristics such as accuracy, precision or steadiness of results in time. The accuracy is related to the estimation bias and can be defined as a measure of proximity between the average estimation result and the ground truth value, while the precision measures the degree of concordance between different realizations obtained under similar circumstances.

2.2.1. Accuracy Index

Considers the relative width of the 95% confidence interval for the EoD estimate at time t (CI_t), when compared to its conditional expectation ($E_t\{EoD\}$) [30]. Equation (2) quantifies the concept of “the more the amount of data, the more accurate the estimation results”.

$$I_1(t) = e^{-\left(\frac{\sup(CI_t) - \inf(CI_t)}{E_t\{EoD\} - t}\right)} \quad (2)$$

$$0 < I_1(t) \leq 1, \forall t \in [1, E_t\{EoD\}], t \in \mathbb{N}$$

Accurate prognosis results are associated to values of $I_1(t) \sim 1$.

2.2.2. Accuracy-precision Index

Represents the amount of bias on the estimation of the EoD time, relative to the width of the corresponding 95% confidence interval, and penalizes the fact that the estimated expected value is greater than the real failure time (ground truth) (Orchard, et al. 2009).

$$I_2(t) = e^{-\left(\frac{\text{GroundTruth}\{EoD\} - E_t\{EoD\}}{\sup(CI_t) - \inf(CI_t)}\right)} \quad (3)$$

$$0 < I_2(t), \forall t \in [1, E_t\{EoD\}], t \in \mathbb{N}$$

Good results of this index are associated to values such that $0 \leq 1 - I_2(t) < \varepsilon$, where ε is a small positive constant.

2.2.3. On-line Steadiness Index

Corresponds to the capacity of the algorithm to deliver prognosis results that are consistent in time. The evolution in time of the EoD conditional expected value is considered, and quantifies the concept “the more amount of data, the more stable the prognosis result should be” (Orchard, et al. 2009).

$$I_3(t) = \sqrt{\text{Var}(E_t\{EoD\})} \quad (4)$$

$$0 \leq I_3(t), \forall t \in \mathbb{N}$$

Steady results are associated with small values of this index.

2.3. Characterization of the State-of-Charge

One of the main difficulties when estimating the SOC is that this parameter cannot be measured directly, and its value has to be obtained indirectly by measuring other parameters (Pattipati, Sankavaram, Pattipati, 2011), (Qingsheng, Chenghui, Naxin, Xiaoping, 2010), (Cadaru, Petreus, Orian, 2009), (Di, Yan, Quin-Wen, 2011). Also, when estimating the SOC parameters such as temperature, rate of charge/discharge, hysteresis, age of the battery and self-discharge effect (Pattipati, et al., 2011). Chemical models for the SOC require many precise measurements for the different model variables (Pattipati, et al., 2011), (Charkhard & Farrokhi, 2011) and for this reason other methods are preferred. In this sense, the most popular methods are the Ampere-hour counter, internal impedance measurement and the open circuit voltage measurement (OCV) (Pattipati, et al., 2011), (Charkhard & Farrokhi, 2011), (Ran, Junfeng, Haiying & Gechen, 2010), (Qingsheng, et al., 2010), (Di, et al., 2011), (Saha, Goebel, Poll & Christophersen, 2009), (Tang, Mao, Lin & Koch, 2011).

The Ampere-hour counter estimates the battery capacity by the integration of the current during the charge/discharge cycle. This method has the advantage that can be implemented on-line. However, it has disadvantages, perhaps the main one is that it only is able to give good results for short periods of time, which leads to a low acceptance (Pattipati, et al., 2011), (Ranjbar, Banaei, Fahimi, 2012). Other disadvantages include the requirement of accurate measurements, the no consideration of the internal impedance losses, and the need to reference a SOC in order to compare the results (typically its maximum nominal capacity), among others (Pattipati, et al., 2011), (Charkhard & Farrokhi, 2011), (Cadar, et al., 2009), (Di, et al., 2011), (Tang, et al., 2011).

The OCV method has the advantage that it doesn't need information prior to the measurements and that it has a direct relation with the SOC: the higher the OCV, the higher SOC (Tang, et al., 2011). Unfortunately, in order to realize this measurement the battery must have a prolonged period of rest (no current circulating) which makes difficult to use in systems where this time is not enough, and makes it hard to use on-line (Pattipati, et al., 2011), (Charkhard & Farrokhi, 2011), (Di, et al., 2011), (Tang, et al., 2011).

More recently, in (Pola et al., 2015) and (Cerdeja et al., 2012), the battery state model is obtained using an empirical scheme considering parts of the electric equivalents and a curve fitting of the voltage discharge curve, with good results obtained. The model of (Pola, et al., 2015) shown in Eq. (5) considers a two state vector (x_1, x_2) where the first variable corresponds to the internal impedance of the battery and the second represents the state of charge in terms relative to its nominal capacity E_{crit} . The observation equation $v(t)$ characterizes the voltage measured during the discharge of the battery, and it is expressed as a function of the parameters v_0, v_L, α, β and γ . These parameters must be estimated off-line in order to obtain good results. The processes noises (ω_1, ω_2) and observation noise (η) are assumed Gaussian. It is important to mention that ω_2 is correlated to η , since the evolution in time of x_2 depends of the voltage measurements.

$$\begin{cases} x_1(t+1) = x_1(t) + \omega_1(t) \\ x_2(t+1) = x_2(t) - v(t) \cdot i(t) \cdot \Delta t \cdot E_{crit}^{-1} + \omega_2(t) \end{cases} \quad (5)$$

$$v(t) = v_L + (v_0 - v_L)e^{\gamma(x_2(t)-1)} + \alpha v_L(x_2(t) - 1) + \dots$$

$$\dots (1 - \alpha)v_L \left(e^{-\beta} - e^{-\beta\sqrt{x_2(t)}} \right) - i(t)x_1(t) + \eta(t)$$

2.4. SOC Estimation and Prognosis

Sequential Monte Carlo methods such as the PF, offer good performance when used in the implementation of estimation and prognosis modules for nonlinear, non-Gaussian systems (Orchard & Vachtsevanos, 2009). There are studies where

these techniques are applied to monitor the SOC and State-of-Health (SOH) of batteries in (Pola, et al., 2015), (Saha, et al., 2009), (Saha & Goebel, 2009), (Dalal, Ma, He, 2011), (Orchard, Tang, Saha, Goebel & Vachtsevanos, 2010) and (He, Williard, Osterman & Pecht, 2011). An alternative to the PF is the UKF, which has also been applied to the same problem (Bole, Daigle, Gorospe & Goebel, 2014). The UKF outstands for its good performance when nonlinear equations are present and its capacity to be implemented computationally in an efficient way (Van Der Merwe & Wan, 2001). Another type of techniques that becomes complimentary to the mentioned algorithms are the OFCLs, since they have been applied to estimation and prognosis problems (Orchard, et al., 2008), (Orchard, 2007) (Orchard, et al. 2009), hence it becomes interesting to analyze its impact.

3. IMPLEMENTATION OF SOC ESTIMATION SCHEMES BASED ON OUTER FEEDBACK CORRECTION LOOPS

3.1. Database description

Voltage and current data used in all experiments correspond to the discharge of a lithium-ion cell, identical to the ones described in (Pola, et al., 2015), and illustrated in the Figure 1. Data correspond to the characterization of usage of an electric vehicle in the city, specifically the Federal Urban Driving Schedule (FUDS), properly scaled for just one battery cell.

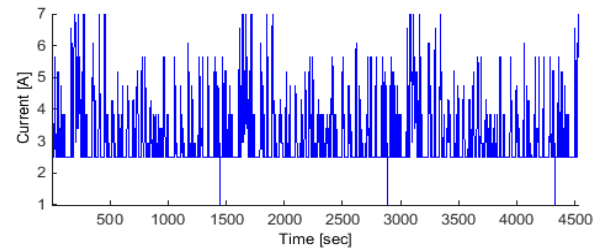


Figure 1 a). Discharge current profile

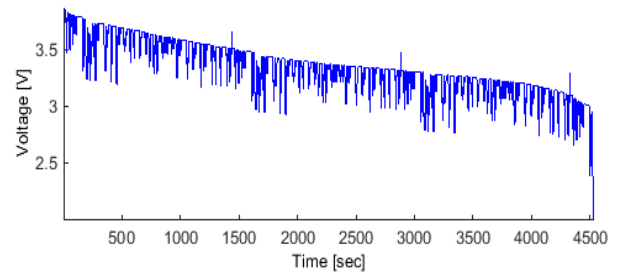


Figure 1 b). Discharge voltage profile

Table 1 shows the values for the parameters of the evolution of the state model. The process and observation noises are assumed Gaussian with a zero mean value.

Table 1. SOC Model Parameter values.

Symbol	Description	Value
E_{crit}	Battery model parameter	46858
Δt	Battery model parameter	1
v_L	Battery model parameter	3.9974
v_0	Battery model parameter	4.144
α	Battery model parameter	0.1469
β	Battery model parameter	17
γ	Battery model parameter	10.4954
R_{ww}	Process noise covariance matrix	$\begin{bmatrix} 0.0015^2 & 0 \\ 0 & 0.0055^2 \end{bmatrix}$
R_{vv}	Observation noise covariance	0.067
r_0	Experimental internal resistance	0.1

3.2. Classical Particle Filter implementation

The base case used for comparison purposes corresponds to the classical PF-based implementation developed in (Pola, et al., 2015). It uses a total of 40 particles and a basic design for an OFCL. The model described in Eq. (5) is used for this scheme.

The basic OFCL implemented in (Pola, et al., 2015) considers a reduction of the process noise associated with the evolution of SOC in time, starting at a fixed time instant and considering a lower bound for the variance. In other words, if $\omega_2(t)$ is the process noise associated to the evolution of the battery SOC in time, then the OFCL is:

$$\text{If: } t > 200 \\ \text{then: } std(\omega_2(t+1)) = \max(std(\omega_2(t))/1.01, 2 \cdot 10^{-4})$$

In this case, $std(\omega_2(t))$ is the standard deviation of the process noise at time t . This belongs to a basic correction loop since it does not measure the prediction capability of the model when using the output of the PF algorithm as the initial condition for prognosis. Instead, it opts to reduce the noise variance under the assumption that there is less uncertainty associated with the state estimation process since the filter has received more information. The PF estimates iteratively the SOC as new measurements of voltage and current are acquired. However, the complete scheme also includes the prognosis of the discharge. By applying the state transition equations, is possible to characterize probabilistically the moment in which the battery is fully discharged (when the SOC falls down under a certain threshold or within a hazard zone). Nevertheless, it

is necessary to know the value of the current that will be demanded in the future. To solve this issue, the work done in (Pola, et al., 2015) proposes a two-state Markov Chain that emulates usage profiles with low and a high discharge currents. These two values, as well as the transition probabilities, are determined from historic measurements of the power demand. A more detailed description can be found in (Cerda et al, 2012). In (Pola, et al., 2015), 25 realizations of discharge current profiles are used for prognosis purposes, hence the discharge time estimate computed at a determined moment corresponds to the weighted sum of 25 empirical distributions (Law of Total Probabilities), where each distribution is computed accordingly to Eq. (6), where H_{lb} and H_{ub} are, respectively, the lower and upper bounds of the hazard zone.

$$\widehat{Pr}(EoD) = \sum_{i=1}^{N_p} \Pr\{H_{lb} \leq x_2(EoD) \leq H_{ub}\} \mathcal{W}_i(EoD) \quad (6)$$

The discharge zone of the cell is defined in terms of a uniformly distributed hazard zone between 5.5% and 4.5% of remaining charge, becoming more critical when particles come near the lower bound. When calculating the distribution of the ToF of the prognosis scheme, the weight of each particle in Eq. (6) is modified as:

$$\mathcal{W}'_i(EoD) = \mathcal{W}_i(EoD) \cdot \min\left(\frac{0.055 - |\hat{x}_{i,2}(ToF)|}{0.055 - 0.045}, 1\right) \quad (7)$$

where $\hat{x}_{i,2}$ corresponds to the estimated value for the second state (SOC) of the i^{th} particle.

3.3. Battery Model

The discharge equations of a lithium-ion cell shown in Eq. (5) have a small inconsistency when compared to a traditional space state model: the evolution of the second state depends on the output of the system. Since the model output is a function of the state and the input, the right manner to implement the battery model is by replacing $v(t)$ by its prior estimate, as shown in Eq. (8). The reason why the model of Eq. (5) is used in (Pola, et al., 2015) is simply because it is computationally less expensive, since it directly uses the acquired measurement instead of calculating the whole expression for each particle. In this approach, the algorithms are developed using the following model in order to describe the evolution of the states:

$$\begin{aligned} x_1(t+1) &= x_1(t) + \omega_1(t) \\ x_2(t+1) &= x_2(t) + \dots \\ &- \left(v_L + (v_0 - v_L)e^{\gamma(x_2(t)-1)} + \alpha v_L(x_2(t) - 1) \right) \\ &+ (1 - \alpha)v_L \left(e^{-\beta} - e^{-\beta\sqrt{x_2(t)}} \right) - i(t)x_1(t) \\ &\quad \cdot i(t) \cdot \Delta t \cdot E_{crit}^{-1} + \omega_2(t) \end{aligned} \quad (8)$$

$$\begin{aligned} v(t) &= v_L + (v_0 - v_L)e^{\gamma(x_2(t)-1)} + \alpha v_L(x_2(t) - 1) + \dots \\ &\dots (1 - \alpha)v_L \left(e^{-\beta} - e^{-\beta\sqrt{x_2(t)}} \right) - i(t)x_1(t) + \eta(t) \end{aligned}$$

3.4. Unscented Kalman Filter

The UKF that is implemented corresponds to the classic version of the algorithm with the exception that the square root of the covariance matrix is replaced by its Cholesky factor, since the calculation is much simpler computationally speaking. Additionally, an outer correction loop is incorporated. The specific values of the UKF can be seen in Table 2.

Table 2. UKF Parameter values.

Symbol	Description	Value
N	Battery model parameter	46858
α	Battery model parameter	1
β	Battery model parameter	3.9974
κ	Battery model parameter	4.144

It is important to mention that in the prognosis stage, the original structure described in (Pola, et al., 2015), which is based on empirical distributions, is maintained. Then, to prognosticate the EoD time it is necessary to sample the Gaussian probability density function (PDF) related to the state estimate. This is achieved by generating a sampling from the multidimensional Gaussian obtained by the UKF to represent the probability density distribution of the state, where each sample corresponds to the position of a particle and the weight is equal to all of the particles.

3.5. Outer Feedback Correction Loops

The implementation of OFCL aims to improve the performance of the estimation module, regardless of the main algorithm that is used for this purpose: UKF or PF. The OFCL designed for this case study affects the standard deviation of the process noise, which is assumed as Gaussian with a mean value of zero. This particular OFCL, though, is not based on short-term prediction results, but on the accumulated observation error instead. By observing the database, the voltage in the battery does not have considerable variations in small intervals of time (less than 30 seconds) during almost all the discharge cycle. Even more, the typical voltage drop that the battery undergoes during small time intervals, due to changes in the SOC, is comparable to the observation noise. In this regard, short-term predictions are not enough to evaluate the performance of the model. Increasing the prediction horizon is not a practical answer to this issue, since this generates algorithms lags and requires more memory. The use of the accumulated observation error solves the problem related to the required memory space; and also allows to evaluate the model performance, since it is able to detect inconsistencies between measurements and estimations of the output in previous time horizons. Thus, the proposed OFCL results:

If: $t > t_{min}$,
then:

$$e_{accum} = e_{accum} + |e_{obs}|$$

If: $e_{accum} \leq e_{Th}$

$$std(\omega_1(t)) = \max(p_1 \cdot std(\omega_1(t)), \underline{std}_1)$$

$$std(\omega_2(t)) = \max(p_2 \cdot std(\omega_2(t)), \underline{std}_2),$$

elseif:

$$e_{accum} = 0$$

$$std(\omega_1(t)) = q_1 \cdot std(\omega_1(t))$$

$$std(\omega_2(t)) = q_2 \cdot std(\omega_2(t))$$

In this case, t_{min} corresponds to the instant in which the OFCL starts operating; e_{obs} is the observation error (the difference between the acquired measurement for the output and the one expected by the estimation algorithm); e_{accum} is a variable that accumulates the past observation errors with initial value of zero; e_{Th} is the decision threshold to modify the process noise. In other words, if it is lower than the threshold, the standard deviation of the process noise is reduced, but if it is larger than the threshold, it increases. Also p_1 and p_2 are constants with values between 0 and 1, while q_1 and q_2 are constants bigger than 1. Finally, \underline{std}_1 and \underline{std}_2 are the lower bounds which indicate the minimum standard deviation accepted value.

It is important to mention that the decision to increase the process noise includes a reset of the accumulated error, in order to allow the algorithm to have a time interval to correct its estimation before continuing to increase the uncertainty. In case that the observations do not meet the likelihood requirements, the accumulated error will become bigger than the threshold and the OFCL will increase the process noises. On the other hand, if small observation errors, accumulated during a prolonged time horizon, are able to surpass the activation threshold, the augmentation of the noise will only be done one time on that time horizon, and its effect will not be determinant on the performance of the method.

Table 3 summarizes the values of the parameters for the correction loops. The numeric differences for both methods are because the nature of each algorithm, basically the PF sensitivity to adjust its estimation, since the particles move quickly towards a zone with more likelihood with the observation. The reason because q_1 has a bigger value than q_2 is the decision of penalizing a higher uncertainty of the internal impedance estimation, since there is not available a good transition model for it.

Table 3. Parameter values for the OFCL in UKF and FP.

Symbol	Description	Value
t_{min}	5	200
e_{rh}	0.15	0.15
p_1	0.99	0.99
p_2	0.98	0.99
q_1	1.1	1.1
q_2	1.01	1.01
std_1	10^{-5}	10^{-4}
std_2	10^{-5}	10^{-4}

3.6. Prognosis Performance

To evaluate the prognosis capability offered by the model and the outcomes of the estimation stage, the indices mentioned in Section 2 are used. Since these indices are functions of time, every value (at each time instant) requires to compute the output of the prognostic routine, conditional to the available information, until the end of the prediction horizon. To lower computational costs, one EoD prognosis result is computed every 10 iterations of the estimation module. When using the UKF within the estimation module, only one execution of the code is required (since it is a deterministic algorithm). However, in the case of PF algorithms, all results consider an average of 30 realizations of the code.

4. RESULTS

This research effort presents a comparison between filtering stages based on either PF or UKF, using OFCLs, and measuring the impact on the subsequent prognosis stage. For completeness purposes, and to measure the impact of OFCLs on filtering stages, we have also included results where classical version of the aforementioned filters are used during the estimation stage. Analysis is focused on estimation and prognosis of battery internal impedance, voltage and SOC. Experimental data were obtained from fully-charged cells (initial SOC is 100%), although initial condition always assumed 85% for the cell SOC to incorporate the effect of incorrect initial conditions.

4.1. PF-based Estimation and Prognosis

To establish a comparison between different estimation algorithms, it becomes convenient to establish a base scenario, which in this case corresponds to a classical implementation of PF-based estimation and prognosis modules. Since one execution of the PF code corresponds to a realization of a stochastic process, all conclusions require

to analyze several realizations of the code. Figures show only one particular realization of the algorithm.

4.1.1. PF-based Estimation Results

Figure 2 shows PF-based estimates of the SOC, internal impedance, and voltage of the lithium-ion cell. The initial SOC of the battery is 100%, while for the PF the initial condition assigned is a uniform random sample between 76.5% and 93.5% (mean value of 85%) to evaluate if the algorithm is capable of correcting errors in the initial conditions. The initial condition assigned to the internal impedance is a Gaussian distribution sample of mean value of 0.1 and a variance of $2.5e-5$. These values were determined experimentally in (Pola, et al., 2015), as shown in Table 1. The set of points plotted around the solid lines correspond to realizations associated with each particle, previous normalization of its weights through resampling.

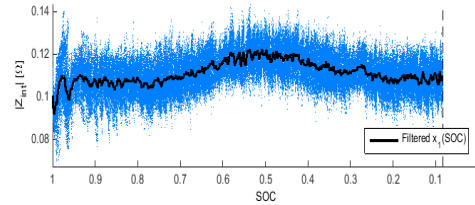


Figure 2 a). PF Internal impedance estimation

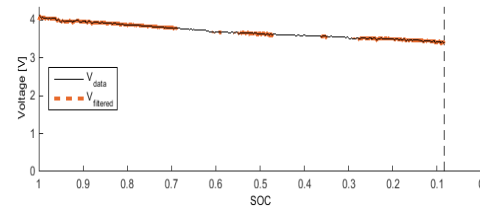


Figure 2 b). PF Voltage measurement and estimation

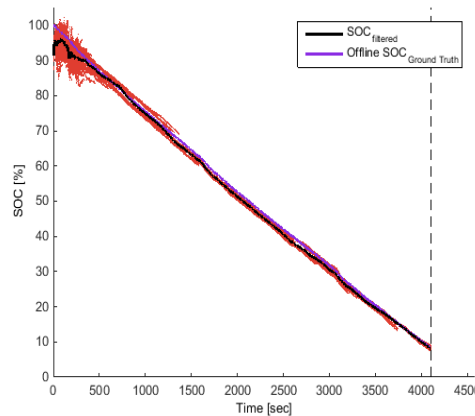


Figure 2 c). PF SOC estimation results

4.1.2. PF-based Prognosis Results

Figure 3 shows one execution of the PF estimation and prognosis routine for a complete discharge cycle. On Figure 3 a), the filtered impedance value can be observed, as well as the value for each particle during the first stage. Later, the prognosis stage assumes that the impedance value is constant, while the 95% confidence level (thinner lines) increases in time. On Figure 3 b), it becomes notorious that the predicted voltage becomes fully discharged before the real data, hence a bad adjustment of the model towards the end of the discharge. Figure 3 c) shows the estimation and prognosis as well as the actual SOC value. Also, the discharge zone and the exact point when the battery is fully discharged (ground truth EoD). Finally, Figure 3 d) presents the probability density distribution for the time of failure or discharge, with a 95% confidence interval.

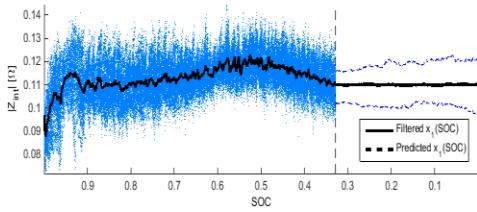


Figure 3 a). PF Internal impedance estimation and prognosis

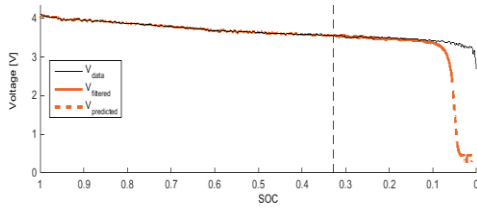


Figure 3 b). PF Voltage estimation and prognosis

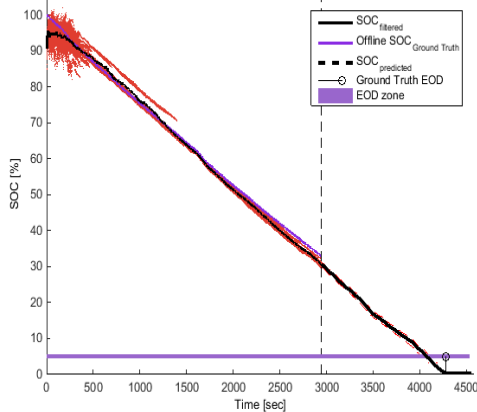


Figure 3 c). PF+OFCLs SOC estimation and prognosis with 95% confidence intervals

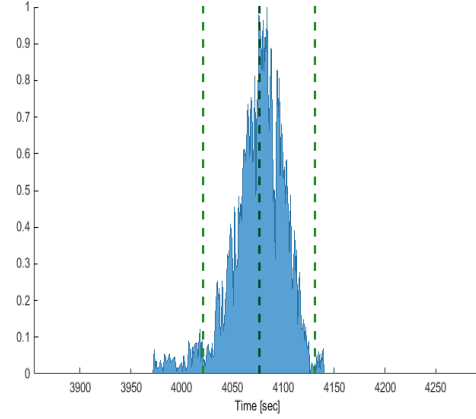


Figure 3 d). PF+OFCLs Prognosis EoD probability density function

It is possible to notice that the procedure allows to implement a satisfactory prognosis scheme, in which no overestimation of the EoD time occurs. Moreover, the uncertainty is characterized in an adequate manner, which translates into a conservative approach.

4.2. Estimation and Prognosis results based on a combination of PF and OFCL

This section presents the results obtained when combining Outer Feedback Correction Loop (OFCLs) with the classical PF implementation. Once again, and since this is a stochastic algorithm, different results are obtained at each realization. Figures illustrate the average performance of the method, without perjury of realizations with better or worse results.

4.2.1. PF+OFCLs Estimation Results

Figure 4 shows the estimation using a PF+OFCLs when the initial SOC is of the battery is 100% and the assumed initial value is 85%. On Figure 4 a) the internal impedance module is shown. Here the dispersion of the particles is smaller, which implicates a smoother behavior.

Also, it is possible to notice on Figure 4 b) the status of the OFCL, and when it switches from “off” to “on”. Finally, Figure 4 c) shows the filtered and the offline SOC. It is possible to notice that the OFCL is able to quickly correct the initial condition, and correctly estimate the SOC ground truth.

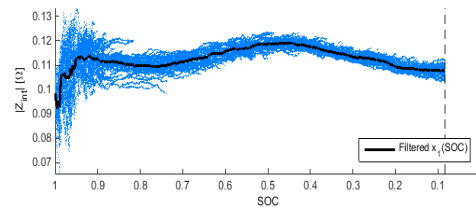


Figure 4 a). Internal impedance estimation

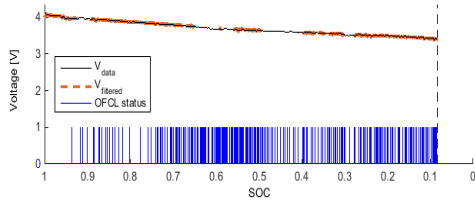


Figure 4 b). PF+OFCLs Voltage measurement and estimation with OFCL

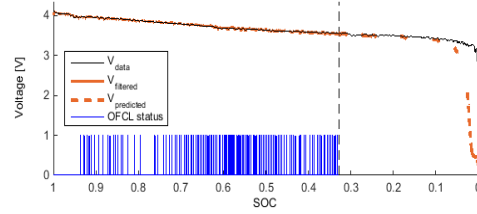


Figure 5 b). PF+OFCLs Voltage estimation and prognosis with OFCL

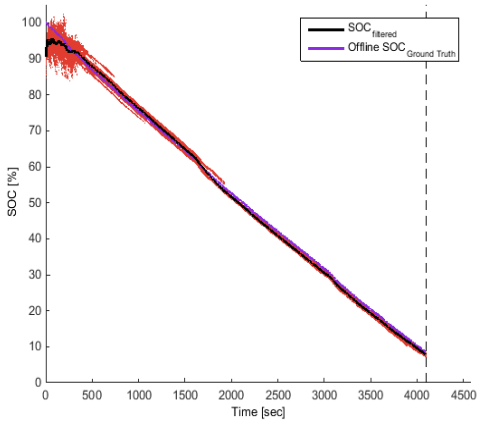


Figure 4 c). PF+OFCLs SOC estimation results

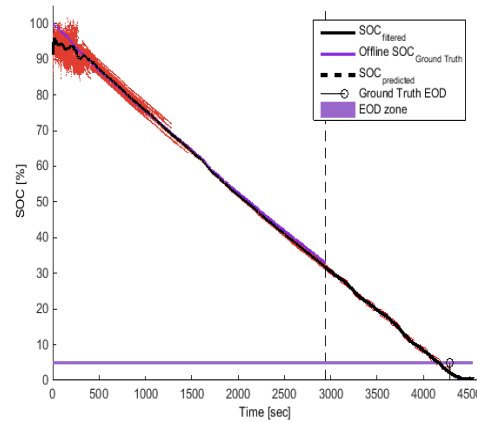


Figure 5 c). PF+OFCLs SOC estimation and prognosis with 95% confidence intervals

4.2.2. PF+OFCL Prognosis Results

The results obtained for this approach are similar when the OFCL was not included. The main difference is shown in Figure 5a), since there is a reduction of the particle dispersion during the estimation stage, translated in a smaller 95% confidence intervals when doing prognosis. Figure 5b) shows the OFCL action. This action is defined as a two possible numbers: a number 1 indicates an increase of the standard deviation of the process noise, and a number 0 indicates a decrease of the same concept due to the good estimation performance. It is possible to note, that the prognosis of the discharge time is more accurate than the previous case. In other words, the distribution of the EoD time is closer to the ground truth.

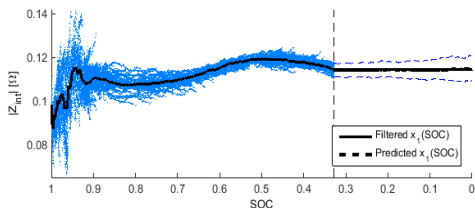


Figure 5 a). PF+OFCLs Internal Impedance estimation and prognosis

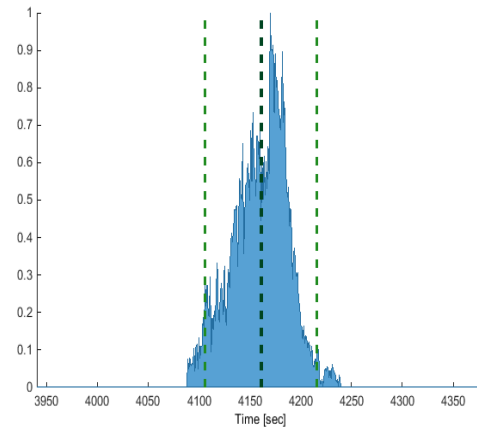


Figure 5 d). PF+OFCL Prognosis EoD probability density function

4.3. UKF Estimation Module

Similarly to the previous case, results for the estimation and prognosis of the internal impedance, voltage, and battery SOC based on UKF schemes are now described. To measure the impact of OFCL on filtering stages, we have also included results where those correction loops were not activated. It is important to note that the UKF is used just for the estimation stage, since the prognostics are obtained using a PF-based scheme. In other words the estimation stage is performed using a UKF-based module, while the prognosis follows a classic PF-based implementation.

4.3.1. UKF Estimation Results

When using the UKF in the estimation module, the initial value of the state vector is characterized through a Gaussian distribution. This is intended to create similar conditions as the ones determined on the PF base scheme. Figure 6 shows the estimation realized with a UKF during one single discharge cycle. The dotted lines correspond to a 95% confidence interval, while the solid line indicates the estimation of the internal impedance and SOC. Figure 6c) shows that even though the UKF estimation quickly converges to actual SOC value during early stages of the algorithm execution, then eventually the filter diverges.

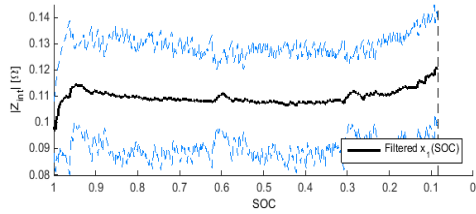


Figure 6 a). UKF Internal impedance estimation

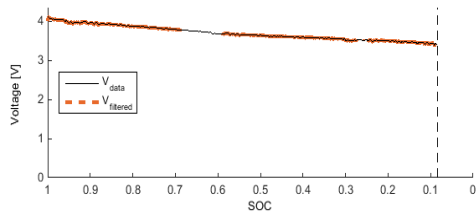


Figure 6 b). UKF Voltage measurement and estimation

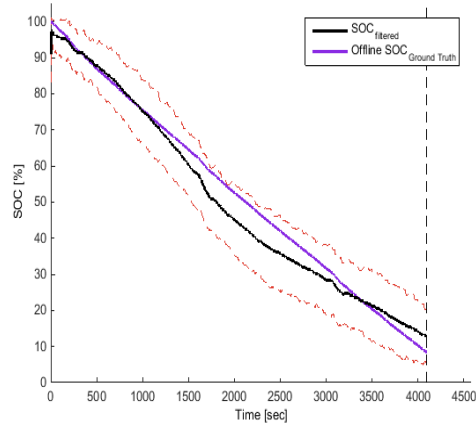


Figure 6 c). UKF SOC estimation results

It is important to mention that this poor performance condition coincides with periods in which larger currents values are demanded from the battery. In this situation, non-modeled dynamics of the battery affect measurements more evidently, reflecting on larger discrepancies for the results of the prognosis module. This fact is also reflected on large variances of the state vector

4.4. Estimation and Prognosis based on a combination of UKF and OFCLs

4.4.1. UKF+OFCLs Estimation Results

The same procedure as before is applied to this new scheme, in which the OFCL is combined with an UKF-based estimation module. Figure 7 shows the results for this framework.

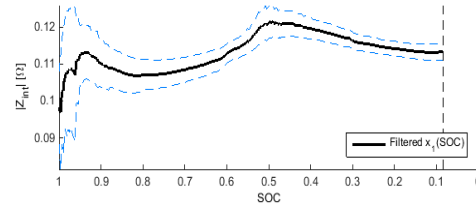


Figure 7 a). UKF+OFCLs Internal impedance estimation

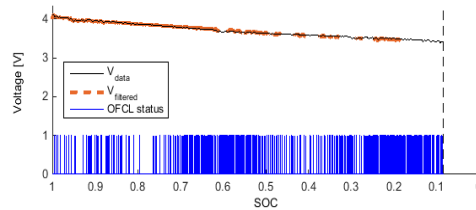


Figure 7 b). UKF+OFCLs Voltage measurement and estimation

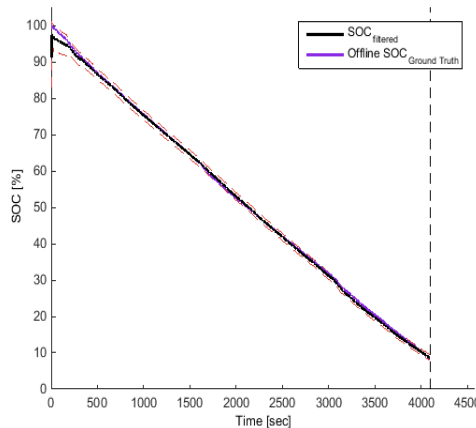


Figure 7 c). UKF+OFCLs SOC estimation results

The addition of the OFCLs improves considerably the performance, thus achieving more accurate SOC estimates.

The reason for which the combination of UKF+OFCLs provides good results is that the empirical model obtained for the Li-Ion cell describes in a good way the real behavior during a large part of the discharge cycle. In this regard, the diminishment of the process noise is a result of the addition of the OFCLs, which allows the UKF to have a bigger robustness to measurements errors and certain flexibility to adapt when the observations do not match the one-step ahead predictions.

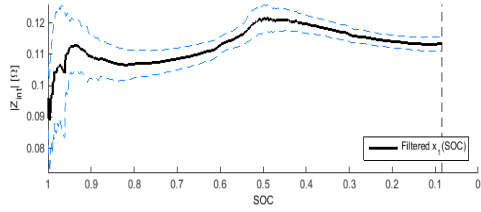


Figure 8 a). UKF+OFCLs Internal impedance estimation

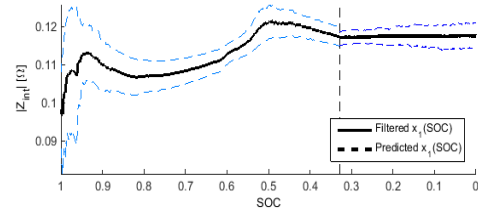


Figure 9 a). UKF+OFCLs Internal impedance estimation and prognosis

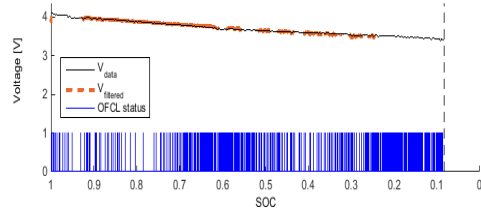


Figure 8 b). UKF+OFCLs Voltage measurement and estimation

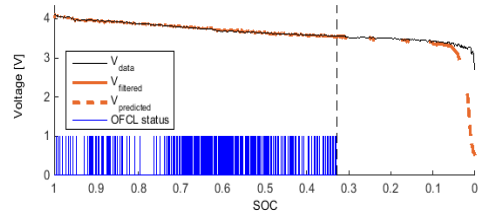


Figure 9 b). UKF+OFCLs Voltage estimation and prognosis with OFCLs

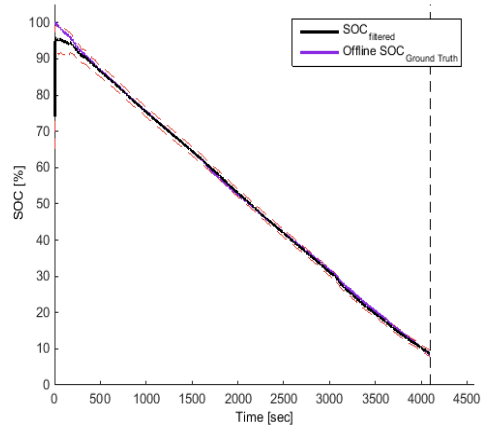


Figure 8 c). UKF+OFCLs SOC estimation results

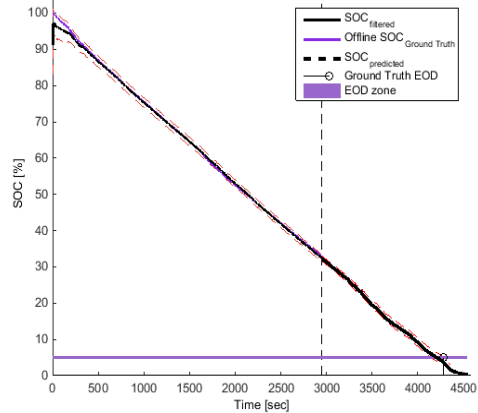


Figure 9 c). UKF+OFCLs SOC estimation and prognosis with 95% confidence intervals

Another factor to consider is the larger variance on the estimation of the state when obtaining voltage measurements that are not similar to the model prediction. This effect can be reduced with a smaller covariance matrix, combined with a smaller process noise associated with the SOC evolution in time, considering the risk that estimates may be biased, since the assumed initial conditions are dissimilar to the actual conditions in the battery.

4.4.2. UKF+OFCL Prognosis Results

Figures 9a) to 9d) show the results for one realization of the prognosis module when using the UKF+OFCLs scheme during the filtering stage. It is possible to note an adequate performance according to what is expected. The results are similar to the ones obtained with the PF and the PF+OFCLs schemes, with the benefit that the accuracy of determining the discharge time is higher, associated to a good previous estimate of the battery SOC.

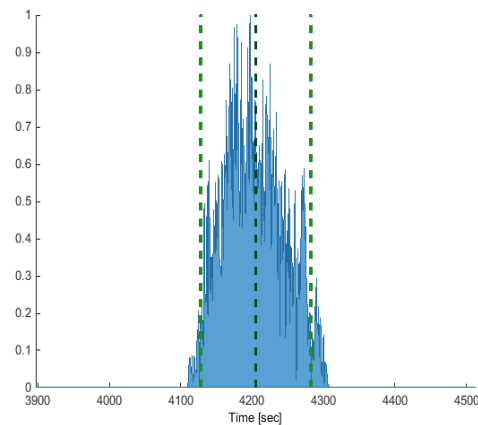


Figure 9 d). UKF+OFCLs Prognosis EoD probability density function

5. PERFORMANCE COMPARISON

Although graphic information is helpful to understand the performance and effectiveness of the different algorithms, it is not enough to evaluate the specific performance from a numeric point of view, so objective comparisons cannot be made. Even more, in the case of PF, one realization is not able to capture its real behavior, making it necessary to use the average of different realizations in order to establish an adequate characterization.

The following results correspond to three estimation experiments. Experiment #1 corresponds to the one shown on the previous figures, where the mean value of the initial condition is 85% of the SOC, while the real value is 100%. Similarly, Experiments #2 and #3 correspond to a SOC of 65% and 50%. Not all these results are shown in this article, since results from Experiments #2 and #3 exhibited similar performance as Experiment #1. The UKF without the OFCLs is left out of the experiments due to its poor performance. For the PF-based algorithms the average of 50 realizations is considered. The measurements were made at four time instants of the discharge period: near the beginning (200 seconds), two at the central area (1200 and 2700 seconds) and near the end (4100 seconds).

Additionally, a prognosis experiment is made where the performance indices explained before are accounted. These indices are time functions, so they require long term predictions at every instant during the whole discharge. To decrease the computational requirements, the predictions are made every 10 iterations. Also, since the computational cost is elevated, the numbers of realizations for the PF are reduced to 30.

5.1. Estimation Stage: 85% SOC initial charge assumed

The Tables 4, 5, 6 show the results for the different schemes. The SOC error is presented with a 95% confidence interval.

Table 4. Experiment #1: PF (average of 50 realizations).

Time	T=200	T=1200
Mean	$\begin{bmatrix} 0.1110 \\ 0.9294 \end{bmatrix}$	$\begin{bmatrix} 0.1115 \\ 0.7105 \end{bmatrix}$
Covariance (10^{-4})	$\begin{bmatrix} 0.0424 & 0.1425 \\ 0.1425 & 0.7990 \end{bmatrix}$	$\begin{bmatrix} 0.3920 & 0.1423 \\ 0.1423 & 0.7519 \end{bmatrix}$
SOC error	0.0200 ± 0.0210	0.0004 ± 0.0203
Time	T=2700	T=4100
Mean	$\begin{bmatrix} 0.1163 \\ 0.3692 \end{bmatrix}$	$\begin{bmatrix} 0.1052 \\ 0.0735 \end{bmatrix}$
Covariance (10^{-4})	$\begin{bmatrix} 0.4081 & 0.0676 \\ 0.0676 & 0.2723 \end{bmatrix}^{10}$	$\begin{bmatrix} 0.3320 & 0.0877 \\ 0.0877 & 0.1937 \end{bmatrix}^{10-4}$
SOC error	0.0105 ± 0.0206	0.0101 ± 0.0219

Table 5. Experiment #1: PF+OFCLs (average of 50 realizations).

Time (s)	T=200	T=1200
Mean	$\begin{bmatrix} 0.1112 \\ 0.9299 \end{bmatrix}$	$\begin{bmatrix} 0.1105 \\ 0.7154 \end{bmatrix}$
Covariance (10^{-4})	$\begin{bmatrix} 0.0404 & 0.1327 \\ 0.1327 & 0.7700 \end{bmatrix}$	$\begin{bmatrix} 0.0643 & 0.1864 \\ 0.1864 & 0.8127 \end{bmatrix}$
SOC error	0.0195 ± 0.0190	-0.0045 ± 0.0090
Time (s)	T=2700	T=4100
Mean	$\begin{bmatrix} 0.1171 \\ 0.3695 \end{bmatrix}$	$\begin{bmatrix} 0.1076 \\ 0.0775 \end{bmatrix}$
Covariance (10^{-4})	$\begin{bmatrix} 0.0275 & 0.0213 \\ 0.0213 & 0.1242 \end{bmatrix}$	$\begin{bmatrix} 0.0318 & 0.0301 \\ 0.0301 & 0.1131 \end{bmatrix}$
SOC error	0.0102 ± 0.0184	0.0062 ± 0.0154

Table 6. Experiment #1: UKF+OFCLs.

Time (s)	T=200	T=1200
Mean	$\begin{bmatrix} 0.1125 \\ 0.9395 \end{bmatrix}$	$\begin{bmatrix} 0.1082 \\ 0.7096 \end{bmatrix}$
Covariance (10^{-4})	$\begin{bmatrix} 0.166 & 0.341 \\ 0.341 & 1.154 \end{bmatrix}$	$\begin{bmatrix} 0.0310 & 0.1012 \\ 0.1012 & 0.4137 \end{bmatrix}$
SOC error	0.0099	0.0013
Time (s)	T=2700	T=4100
Mean	$\begin{bmatrix} 0.1191 \\ 0.3766 \end{bmatrix}$	$\begin{bmatrix} 0.1134 \\ 0.0860 \end{bmatrix}$
Covariance (10^{-4})	$\begin{bmatrix} 0.0187 & 0.0493 \\ 0.0493 & 0.2602 \end{bmatrix}$	$\begin{bmatrix} 0.0141 & 0.0373 \\ 0.0373 & 0.1716 \end{bmatrix}$
SOC error	0.0030	-0.0023

It is possible to note that the use of the OFCLs generates more accurate (smaller error) and more precise (smaller variance) estimations than the base PF used for comparison. In particular, the UKF+OFCLs is the algorithm with the highest accuracy, although its inability to represent multimodal distributions as the ones observed on the results. It is important to mention the considerable reduction of the variance of the internal impedance estimation module.

5.2. Performance measures

This section presents results obtained in terms of the evaluation of performance indices such as: precision, accuracy-precision, and on-line steadiness for prognosis. Figures 10a) to 10c) show the obtained values of the aforementioned performance indices, for the following cases: Base PF, PF+OFCLs and UKF+OFCLs.

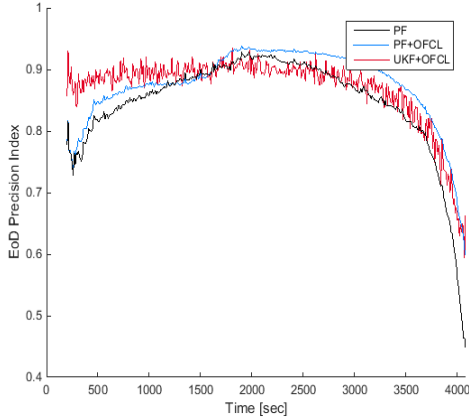


Figure 10 a). EoD Precision Index

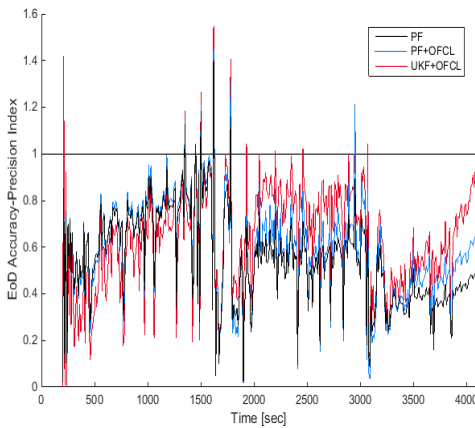


Figure 10 b). EoD Accuracy-Precision Index

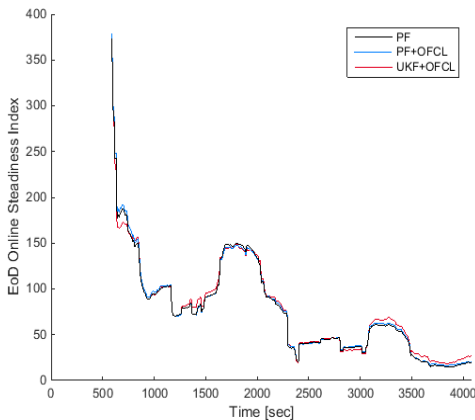


Figure 10 c). EoD online Steadiness Index

The PF+OFCLs has a notorious improvement in its precision and accuracy-precision indices when compared to the base case. However the UKF+OFCLs scheme is the one that presents better performance. From the Accuracy-Precision index, it becomes clear that is the only scheme with a tendency to the value of 1, when the end of the discharge is almost complete. In other words, the predicted EoD is smaller with every time instant that passes.

6. CONCLUSIONS

Even though the UKF has a Square-Root version, which is reported as computationally more stable, and more efficient in times, this variant is not convenient for the treated problem. The realized implementations showed a more elevated execution time, given the model dimensionality. That is to say, for a two state characterization it is more efficient to calculate at each iteration of the UKF la square root of a matrix, which can be done with a Cholesky decomposition or in the analytical way for case of 2×2 matrices.

The effectiveness of the programmed algorithms (performance in estimation and prognosis) is improved when the OFCLs are incorporated in all cases of study. The UKF without the OFCL has a poor performance, and is not recommended, but if the OFCL is added, the performance is even better than the PF schemes, as long as there is a reliable model. This means that the process and ideally the observation noises have to be small enough or be able to allow its diminishment through OFCLs.

The results of the UKF are favored since the observation model and the state transition have a mainly linear behavior during the intermediate part of the discharge.

The PF schemes, with or without the OFCLs have acceptable results with SOC estimation errors that are below a 4% of the real value, except when the assumed and real initial condition are very different. The proposed structure of OFCLs allows an improvement on the performance of the different estimation algorithms. This means that the accumulated observation error is a useful index to make decisions of how to modify the model hyper parameters. This means that when facing a SOC estimation problem, it is highly recommended to start the study with a PF scheme to verify that the model is able to describe the phenomenology of the battery. If good results are obtained, the implementation of an UKF+OFCLs can help improve the consistency and quality of the results, and even the execution time depending on the platform that is implemented.

ACKNOWLEDGEMENTS

This work has been partially supported by FONDECYT Chile Grant Nr. 1140774, and the Advanced Center for Electrical and Electronic Engineering, Basal Project FB0008. The work of Jorge Silva was supported by CONICYT-Chile, FONDECYT Chile Grant Nr. 1140840. The work of Aramis Pérez was supported by the University of Costa Rica (Grant for Doctoral Studies) and CONICYT-PCHA/Doctorado Nacional/2015-21150121. The work of Vanessa Quintero was supported by the Universidad Tecnológica de Panama and IFARHU (Grant for Doctoral Studies). The work of Francisco Jaramillo was supported by CONICYT-PCHA/Doctorado Nacional/2014-21140201.

REFERENCES

- Bole, B. D. (2014). Online Prediction of Battery Discharge and Estimation of Parasitic Loads for an Electric Aircraft. *Second European Conference of the Prognostics and Health Management Society 2014*, 23-32.
- Cadar, D. P. (2009). method of determining a lithium-ion battery's state of charge. *de 2009 15th International Symposium for Design and Technology of Electronics Packages (SIITME)*.
- Cerda, M. (2012). Estimación en línea del tiempo de descarga de baterías de ion-litio utilizando caracterización del perfil de utilización y métodos secuenciales de Monte Carlo. *M.S. Thesis, Universidad de Chile*.
- Charkhgard, M. &. (2010). State-of-charge estimation for lithium-ion batteries using neural networks and EKF. *IEEE Trans. on Industrial Electronics*, vol. 57, n° 12,, 4178-4187.
- Cruse, T. (2004). Probabilistic Systems Modeling and Validation. *HCF*.
- Dalal, M. M. (2011). Lithium-ion battery life prognostic health management system using particle filtering framework. *Proceedings of the Institution of Mechanical Engineers, Part O: Journal of Risk and Reliability*, vol. 225, n° 1, 81-90.
- Di Z., Y. M.-W. (2011). Estimation of Lithium-ion battery state of charge. *30th Chinese Control Conference (CCC)*.
- He, W. W. (2011). Remaining useful performance analysis of batteries. *IEEE Conference on Prognostics and Health Management (PHM)*.
- Orchard, M. (2007). A Particle Filtering- based Framework for On-line Fault Diagnosis and Failure Prognosis. *Ph.D. Thesis, Department of Electrical and Computer Engineering, Georgia Institute of Technology*.
- Orchard, M. K. (2008). Advances in Uncertainty Representation and Management for Particle Filtering Applied to Prognostics. *International Conference on Prognostics and Health Management PHM 2008*.
- Orchard, M. T. (2009). Outer Feedback Correction Loops in Particle Filtering-based Prognostic Algorithms: Statistical Performance Comparison. *Studies in Informatics and Control*, vol. 18, n° 4, 295-304.
- Orchard, M. T. (2010). Risk-sensitive particle-filtering-based prognosis framework for estimation of remaining useful life in energy storage devices. *Studies in Informatics and Control*, vol. 19, n° 3, 209-218.
- Pattipati, B. S. (2011). System identification and estimation framework for pivotal automotive battery management system characteristics. *IEEE Trans. on Systems, Man, and Cybernetics, Part C: Applications and Reviews*, vol. 41, n° 6,, 869-884.
- Pola, D. N. (2014). Particle-filtering-based Discharge Time Prognosis for Lithium-Ion Batteries with a Statistical Characterization of Use Profiles. *IEEE Transactions on Reability*, 1-11.
- Qingsheng, S. C. (2010). Battery State-Of-Charge estimation in Electric Vehicle using Elman neural network method. *29th Chinese Control Conference (CCC)*.
- Ran, L. J. (2010). Prediction of state of charge of lithium-ion rechargeable battery with electrochemical impedance spectroscopy theory. *the 5th IEEE Conference on Industrial Electronics and Applications*.
- Ranjbar, A. H. (2012). Online Estimation of State of Charge in Li-Ion Batteries Using Impulse Response Concept. *IEEE Trans. on Smart Grid*, vol. 3, n° 1,, 360-367.
- Saha, B. G. (2009). Modeling Li-ion battery capacity depletion in a particle filtering framework. *Proceedings of the annual conference of the prognostics and health management society*.
- Saha, B. G. (2009). Prognostics methods for battery health monitoring using a Bayesian framework. *IEEE Transactions on Instrumentation and Measurement*, vol. 58, n° 2, 291-296.
- Tang, X. M. (2011). Li-ion battery parameter estimation for state of charge. *American Control Conference (ACC)*.
- Van Der Merwe, R. &. (2001). The square-root unscented Kalman filter for state and parameter-estimation. *Acoustics, Speech, and Signal Processing. IEEE International Conference on*, 3461- 3464 vol.6 .

BIOGRAPHIES

B. Sc. Carlos Tampier received the B.Sc. degree in Electrical Engineering from Universidad de Chile, Santiago, Chile, in 2015. Currently he is a researcher at the Advanced Mining Technology Center (AMTC) of the University of Chile. His research interests include control systems, data analysis and machine learning with applications to robotics.

M. Sc. Aramis Pérez is a Research Assistant at the Lithium Innovation Center (Santiago, Chile) and Professor at the School of Electrical Engineering at the University of Costa Rica. He received his B.Sc. degree (2002) and Licentiate degree (2005) in Electrical Engineering from the University of Costa Rica. He received his M.Sc. degree in Business Administration with a General Management Major (2008) and also he is a M.Sc. candidate in Industrial Engineering from the same

university. Currently he is a doctorate student at the Department of Electrical Engineering at the University of Chile under Dr. Marcos E. Orchard supervision. His research interests include parametric/non-parametric modeling, system identification, data analysis, machine learning and manufacturing processes.

B. Sc. Vanessa Quintero received her B.Sc degree from Electronics and Telecommunication Engineering at the Universidad Tecnologica de Panama (2007). Currently she is a doctorate student at the University of Chile. Her research interests include estimation, prognostics with applications to battery and protocols design.

B. Sc. Francisco Jaramillo received the B.Sc. degree in Electronics Engineering from Universidad de La Frontera, Temuco, Chile, in 2009. Currently he is a doctorate student at the Department of Electrical Engineering at the University of Chile under Dr. Marcos E. Orchard supervision. His research interests include machine learning, control systems, and estimation and prognosis based on Bayesian algorithms with applications to nitrogen removal in pilot-scale Sequencing Batch Reactors for Wastewater Treatment Plants.

Dr. Marcos E. Orchard is Associate Professor with the Department of Electrical Engineering at Universidad de Chile and was part of the Intelligent Control Systems Laboratory at The Georgia Institute of Technology. His current research interest is the design, implementation and testing of real-time frameworks for fault diagnosis and failure prognosis, with applications to battery

management systems, mining industry, and finance. His fields of expertise include statistical process monitoring, parametric/non-parametric modeling, and system identification. His research work at the Georgia Institute of Technology was the foundation of novel real-time fault diagnosis and failure prognosis approaches based on particle filtering algorithms. He received his Ph.D. and M.S. degrees from The Georgia Institute of Technology, Atlanta, GA, in 2005 and 2007, respectively. He received his B.S. degree (1999) and a Civil Industrial Engineering degree with Electrical Major (2001) from Catholic University of Chile. Dr. Orchard has published more than 50 papers in his areas of expertise.

Dr. Jorge F. Silva is Associate Professor at the Department of Electrical Engineering, University of Chile, Santiago, Chile. He received the Master of Science (2005) and Ph.D. (2008) in Electrical Engineering from the University of Southern California (USC). He is IEEE member of the Signal Processing and Information Theory Societies and he has participated as a reviewer in various IEEE journals on Signal Processing. Jorge F. Silva is recipient of the Outstanding Thesis Award 2009 for Theoretical Research of the Viterbi School of Engineering, the Viterbi Doctoral Fellowship 2007-2008 and Simon Ramo Scholarship 2007-2008 at USC. His research interests include: non-parametric learning; sparse signal representations, statistical learning; universal source coding; sequential decision and estimation; distributive learning and sensor networks.